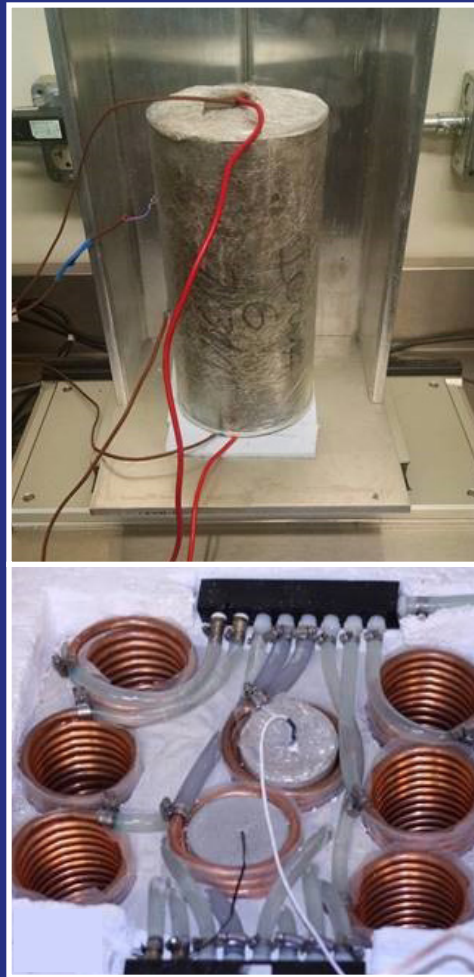


# JOINT TRANSPORTATION RESEARCH PROGRAM

INDIANA DEPARTMENT OF TRANSPORTATION  
AND PURDUE UNIVERSITY



## Implementing Rapid Durability Measure for Concrete Using Resistivity and Formation Factor



**W. Jason Weiss, Chunyu Qiao, Burkan Isgor, Jan Olek**

## RECOMMENDED CITATION

Weiss, J. W., Qiao, C., Isgor, B., & Olek, J. (2020). *Implementing rapid durability measure for concrete using resistivity and formation factor* (Joint Transportation Research Program Publication No. FHWA/IN/JTRP-2020/08). West Lafayette, IN: Purdue University. <https://doi.org/10.5703/1288284317120>

## AUTHORS

### **W. Jason Weiss, PhD**

Professor and Head of Civil Engineering  
Edwards Distinguished Chair in Engineering  
School of Civil and Construction Engineering  
Oregon State University  
*Principal Investigator*

### **Chunyu Qiao, PhD**

Postdoctoral Research Associate  
Oregon State University

### **Burkan Isgor, PhD, PE**

Professor of Civil Engineering and Materials Science  
Oregon State University

### **Jan Olek, PhD, PE**

James H. and Carol H. Cure Professor in Civil Engineering  
Lyles School of Civil Engineering  
Purdue University  
(765) 494-5015  
[olek@purdue.edu](mailto:olek@purdue.edu)  
*Corresponding Author*

## JOINT TRANSPORTATION RESEARCH PROGRAM

The Joint Transportation Research Program serves as a vehicle for INDOT collaboration with higher education institutions and industry in Indiana to facilitate innovation that results in continuous improvement in the planning, design, construction, operation, management and economic efficiency of the Indiana transportation infrastructure. [https://engineering.purdue.edu/JTRP/index\\_html](https://engineering.purdue.edu/JTRP/index_html)

Published reports of the Joint Transportation Research Program are available at <http://docs.lib.purdue.edu/jtrp/>.

## NOTICE

The contents of this report reflect the views of the authors, who are responsible for the facts and the accuracy of the data presented herein. The contents do not necessarily reflect the official views and policies of the Indiana Department of Transportation or the Federal Highway Administration. The report does not constitute a standard, specification or regulation.

## TECHNICAL REPORT DOCUMENTATION PAGE

<b>1. Report No.</b> FHWA/IN/JTRP-2020/08	<b>2. Government Accession No.</b>	<b>3. Recipient's Catalog No.</b>	
<b>4. Title and Subtitle</b> Implementing Rapid Durability Measure for Concrete Using Resistivity and Formation Factor	<b>5. Report Date</b> April 2020		<b>6. Performing Organization Code</b>
	<b>7. Author(s)</b> W. Jason Weiss, Chunyu Qiao, Burkan Isgor, and Jan Olek		
<b>9. Performing Organization Name and Address</b> Joint Transportation Research Program Hall for Discovery and Learning Research (DLR), Suite 204 207 S. Martin Jischke Drive West Lafayette, IN 47907	<b>8. Performing Organization Report No.</b> FHWA/IN/JTRP-2020/08		<b>10. Work Unit No.</b>
	<b>11. Contract or Grant No.</b> SPR-4003-1		
<b>12. Sponsoring Agency Name and Address</b> Indiana Department of Transportation (SPR) State Office Building 100 North Senate Avenue Indianapolis, IN 46204	<b>13. Type of Report and Period Covered</b> Final Report		<b>14. Sponsoring Agency Code</b>
	<b>15. Supplementary Notes</b> Conducted in cooperation with the U.S. Department of Transportation, Federal Highway Administration.		
<b>16. Abstract</b> The durability of in-place concrete is a high priority issue for concrete pavements and bridges. Several studies have been conducted by INDOT to use electrical resistivity as a measure of fluid transport properties. Resistivity is dependent on the chemistry of the cement and supplementary cementitious system used, as such it has been recommended that rather than specifying resistivity it may be more general to specify the formation factor. Samples were tested to establish the current levels of performance for concrete pavements in the state of Indiana. Temperature and moisture corrections are presented and acceptable accelerated aging procedure is presented. A standardized testing procedure was developed (AASHTO TP 119–Option A) resulting in part from this study that provides specific sample conditioning approaches to address pore solution composition, moisture conditioning, and testing procedures. An accelerated aging procedure is discussed to obtain later age properties (91 days) after only 28 days.			
<b>17. Key Words</b> concrete, durability, formation factor, resistivity	<b>18. Distribution Statement</b> No restrictions. This document is available through the National Technical Information Service, Springfield, VA 22161.		
<b>19. Security Classif. (of this report)</b> Unclassified	<b>20. Security Classif. (of this page)</b> Unclassified	<b>21. No. of Pages</b> 24	<b>22. Price</b>

## EXECUTIVE SUMMARY

### Introduction

Ensuring adequate durability of in-place concrete is a high priority. Several studies have been conducted by INDOT to use resistivity as a measure of fluid transport- or permeability-related properties. Resistivity has been shown to be dependent on the chemistry of the pore solution. Formation factor is a more fundamental measure of transport properties and can be obtained experimentally by normalizing the resistivity of the concrete by its pore solution resistivity. A procedure has been developed (AASHTO TP-119-19 Option A) to enable an apparent formation factor to be determined, since the moisture condition is well defined and the pore solution composition is known ( $0.127 \Omega\text{m}$ ). An accelerated aging procedure is described in this report. This project aligns INDOT pioneering work with the national-level efforts (such as those of AASHTO TP-119-19 Option A and AASHTO PP-84-16). This project can benefit the Indiana Department of Transportation (INDOT) with a potential specifiable property which can improve the quality of concrete obtained in the field.

### Findings

This project has several findings including the following:

- Resistivity can be measured using AASHTO TP-119-19 (Option A). This testing procedure was developed based on the findings from INDOT studies and other related studies.
- Samples were tested to establish the current levels of performance for concrete pavements in the state of Indiana.
- Sample conditioning indicates that submerging samples in a simulated pore solution enables the matrix saturation to be reached. This measures transport through the matrix. These findings are consistent with AASHTO TP-119-19 Option A.

- Field samples were tested and may indicate that high paste contents can have a greater connectivity due to the increased porosity of the concrete. It is also noted that concrete with a very low paste content can have an increase in connectivity, presumably due to the connection of the interfacial transition zones and potentially insufficient consolidation.
- Testing can be conducted using a procedure of holding the sample at  $23^{\circ}\text{C}$  for 3 days, followed by 25 days at  $50^{\circ}\text{C}$  to achieve an equivalent age of 91 days. The use of this procedure enables the reactions of supplementary materials to be more fully considered.
- A methodology is reviewed whereby the formation factor can be related to the apparent diffusion coefficient if chloride binding is considered. This could be utilized to establish service life for concrete used in reinforced elements like bridge decks.
- AASHTO PP-84-16 recommends a formation factor of 1,000 for concrete paving mixtures exposed to deicing salts. As such, it is recommended that when AASHTO TP-119-19 Option A is used for testing the trial batch target a resistivity value of  $14.8 \text{ k}\Omega\cdot\text{cm}$  or greater is achieved, while the acceptance value for resistivity used during construction should be  $12.7 \text{ k}\Omega\cdot\text{cm}$  or greater.

### Implementation

This research has been instrumental in the development of standard procedures that have been accepted by AASHTO as AASHTO TP-119-19. INDOT can implement the measurement of resistivity and specification of formation factor using this test. Further, this procedure outlines an accelerated aging procedure. Findings of this research have been presented at several SAC meetings as well as at the national concrete consortium. National studies are underway to assess precision and bias for AASHTO TP-119-19.

## CONTENTS

1. BACKGROUND . . . . .	1
2. RESEARCH OBJECTIVES AND PLAN . . . . .	1
3. WHY SPECIFY FORMATION FACTOR AND NOT RESISTIVITY . . . . .	1
4. SAMPLE CONDITIONING OVERVIEW . . . . .	1
4.1 Sample Geometry . . . . .	1
4.2 Sample Conditioning—Submersion in Pore Solution . . . . .	2
4.3 Sample Conditioning—Temperature Correction . . . . .	2
4.4 Sample Conditioning—Maturity or Aging . . . . .	3
5. REVIEW OF MEASURED RESISTIVITY AND FORMATION FACTORS . . . . .	5
5.1 Porosity . . . . .	5
5.2 Electrical Resistivity . . . . .	5
5.3 Thermogravimetric Analysis (TGA) . . . . .	6
5.4 Low Temperature Differential Scanning Calorimetry (LT-DSC) . . . . .	7
6. ESTABLISH TESTING TIMES FOR THE ACCELERATED TESTING PROCEDURES . . . . .	9
7. ESTABLISHED FORMATION FACTORS FOR PAVEMENTS . . . . .	11
8. ESTABLISHED FORMATION FACTORS FOR OTHER ELEMENTS . . . . .	13
9. REPORTING ACCELERATED TESTING PROCEDURES . . . . .	14
10. SUMMARY OF FINDINGS . . . . .	14
REFERENCES . . . . .	15

## LIST OF TABLES

Table	Page
<b>Table 5.1</b> The Mixture Proportion of the Concrete Cores (lb/yd <sup>3</sup> )	5
<b>Table 7.1</b> Relationship Between Results of the RCPT Test, the Saturated Formation Factor, and the Saturated Resistivity	12
<b>Table 7.2</b> Relationship Between Results of the RCPT Test, the Apparent Formation Factor, and the Apparent Resistivity (Degree of Saturation Has Been Assumed to Be 70%)	12

## LIST OF FIGURES

Figure	Page
<b>Figure 4.1</b> Ratio of the resistivity of concrete at an arbitrary temperature and the resistivity measured at a standard temperature (23°C) based on Equation 4.3	3
<b>Figure 4.2</b> Correction for hydration at different temperatures based on Equation 4.4	4
<b>Figure 5.1</b> Porosity of concrete pavement cores	5
<b>Figure 5.2</b> Electrical resistivity of concrete pavement cores	6
<b>Figure 5.3</b> Formation factor of concrete pavement cores	6
<b>Figure 5.4</b> Pore network connectivity of concrete pavement cores	6
<b>Figure 5.5</b> Relationship between the $\text{Ca(OH)}_2$ content and the amount of formed CAOXY	8
<b>Figure 6.1</b> Temperature profile of the accelerated curing condition	9
<b>Figure 6.2</b> Equivalent age as a function of activation energy	10
<b>Figure 6.3</b> Temperature profile of the accelerated curing condition in ASTM C1202	10
<b>Figure 6.4</b> Equivalent age as a function of activation energy using the accelerated curing procedure in ASTM C 1202	11
<b>Figure 7.1</b> The ratio of the formation factor and apparent formation factor as a function of the degree of saturation	12
<b>Figure 8.1</b> Predicted time to corrosion: (a) influence of cover thickness (b) variability in the percentage of elements requiring repair	13

## 1. BACKGROUND

The durability of in-place concrete is a high priority for INDOT as it relates to concrete pavements and bridges. Several studies have been conducted by INDOT to improve the way that properties related to durability are measured (Spragg et al., 2011). Specifically, several recent research projects have been performed on the use of resistivity as a measure of fluid transport properties (McCarter et al., 1981; Presuel-Moreno et al., 2009; Spragg et al., 2013). While this approach is very positive and able to be implemented in the quality control applications, resistivity is dependent on the chemistry of the cement and supplementary cementitious materials used in making the concrete. As such, it is recommended that rather than specifying resistivity it may be more general to specify the formation factor  $F$  (Weiss et al., 2016). Research has indicated that INDOT can measure the formation factor a variety of ways (Rajabipour et al., 2005; Spragg, 2013). It is recommended that that placing samples in simulated pore solution is a simple method that INDOT can utilize moving forward. This method is referred to in this report as AASHTO TP-119-19 Option A.

## 2. RESEARCH OBJECTIVES AND PLAN

This report includes the following items. First, the measurement of resistivity and formation factor are reviewed. Second, the influence of sample geometry, temperature, and moisture on resistivity measurements are reviewed. Third, concrete samples from concrete pavements in Indiana are tested to establish the current levels of performance for concrete pavements in the state of Indiana. Fourth, an acceptable accelerated aging procedure was outlined for use in acceptance testing. This approach attempts to balance the fact that that contractors prefer early measures of performance for pay adjustment determination while INDOT will likely want to use longer term values that account for the reactions of supplementary materials and hydration. Fifth, AASTHO T 277 criteria are compared with apparent resistivity and formation values. Finally, an approach is outlined that can use the formation factor to predict service life of reinforced concrete elements.

## 3. WHY SPECIFY FORMATION FACTOR AND NOT RESISTIVITY

One goal of this work was to examine how specifications can be developed for concrete using measures related to the electrical properties of concrete. To begin, it should be stated that many groups are advocating for specifications based on resistance, resistivity, or some other measure of these (for example coulombs such as AASTHO T 277 or ASTM C1202). It is the authors' position that formation factor is the correct value to specify since it is inversely related to the product of

porosity and connectivity of the pore structure. As such, the formation factor is a true material property and is independent of the pore solution chemistry or the chemistry of the cement and supplementary cement.

## 4. SAMPLE CONDITIONING OVERVIEW

There are several factors that have been identified as being important to the measurement of electrical properties of concrete. These are summarized below and described in the following section.

- First, resistance is the property measured and resistivity is computed by correcting for the sample geometry. Resistivity is a measured value that is independent of specimen geometry and electrode configuration.
- Second, the conditioning of the samples is incredibly important. This report will recommend that the samples are stored in a simulated pore solution (AASHTO TP-119-19, Option A) for two reasons. First, this enables the matrix pores to be saturated while the air voids remain empty. The authors believe that this is both easily attained more representative of field concrete than vacuum saturation (Moradillo, 2019). Second, by using a calcium hydroxide saturated simulated pore solution the leaching of calcium hydroxide and alkalis from the pore solution (an important component that defines the resistivity of the pore solution) is minimized. Third, by fixing the chemistry of the pore solution the formation factor can be easily computed.
- Third, the use of AASHTO TP-119-19, Option A reduces variability of the resistivity measurement since variability introduced by variations in the air content is eliminated (Moradillo et al., 2019; Spragg et al., 2016).
- Fourth, the temperature at which the samples are tested is very important. A testing procedure has been developed (and a large number of concrete samples were tested to determine an activation energy of conduction (resistivity) of 15.8 kJ/mol (Coyle et al., 2018).

### 4.1 Sample Geometry

Resistivity is a material property that is independent of specimen geometry and electrode configuration. Fundamentally, commercially available devices measure the resistance of the concrete. To obtain resistivity, the measured resistance is corrected for specimen size and electrode configuration. Spragg et al. (2013) described how the correction can be made using a geometry factor for several common geometries using Equation 4.1:

$$\rho = R \cdot k \quad (\text{Eq. 4.1})$$

where  $\rho$  is the resistivity,  $R$  is the measured resistance, and  $k$  is a geometry factor. Spragg et al. (2013) described how the geometry factor can be determined experimentally by comparing to measurement of a solution of known resistivity or how the geometry factor could be determined numerically. Further, Spragg et al. (2013)



provides geometric correction factors for several common geometries. Most notably this includes the uniaxial, four-point surface (Wenner), and embedded rod geometries. It is recommended that INDOT utilize the uniaxial test which has a benefit of a more uniform current distribution throughout the sample (AASHTO TP-119-19) which results in more consistent results and a lower impact of the concrete surface condition. For the uniaxial configuration, the geometry factor  $k$  is computed using Equation 4.2:

$$k = \frac{A}{L} \quad (\text{Eq. 4.2})$$

where  $A$  is the cross-sectional area of the specimen and  $L$  is the length of the specimen or the distance between the metal plates. While this is most frequently utilized on cylinders in the U.S. it can also be applied to cubes or prisms. Spragg et al. (2013) also recommend a procedure for accounting for errors introduced by the medium used to connect the electrodes to the sample (typically sponges saturated with lime water).

It should be noted that surface resistivity can also be measured (AASHTO T 358); however, proper corrections are required for geometry. Spragg et al. (2013) provides an indication of how to perform these geometric corrections. It has been noticed that in several studies incorrect geometry factors are applied (or omitted) resulting in complications in interpreting the data which indicates the importance of making sure this is done properly.

#### 4.2 Sample Conditioning—Submersion in Pore Solution

Based on INDOT research a recommendation was made to AASHTO in 2016 for a specification for uniaxial resistivity testing that is referred to as AASHTO TP-119-19. This testing specification was modified based on the results of this research to include three conditioning procedures have been proposed and approved during 2019 (AASHTO TP-119-19):

- Option A—placing the sample in a bucket of pore solution (Spragg et al., 2016).
- Option B—measuring resistivity for a sealed sample as performed in SPR-3752 (Barrett et al., 2015).
- Option C—vacuum saturating a sample to provide a comparison to measures like ASTM 1202.

While INDOT could utilize any of these methods, it is currently being recommended that Option A be utilized. Option A consists of immersion of specimens in a calcium hydroxide-saturated, simulated pore solution.

Option A requires that two 100-mm × 200-mm specimens are submersed in a single 5-gallon bucket with approximately 38 mm of solution covering the samples. The solution is a calcium hydroxide-saturated, simulated pore solution. The calcium hydroxide-saturated, simulated pore consists of 7.6 g/L NaOH (0.19 M); 10.64 g/L KOH (0.19 M); 2 g/L Ca(OH)<sub>2</sub> (all chemicals should be reagent grade materials). The solution can be made using 13,250.0 g water, 102.6 g NaOH, 143.9 g KOH and 27.0 g Ca(OH)<sub>2</sub>. While the previous “recipes” for solution are useful, the key parameter is that when complete resistivity of the simulated pore solution is 0.127 Ω m. It is recommended that sample are placed in the solution immediately after demolding at 1 day and no measurements are taken before 6 days in solution to allow the sample to approach a steady state of pore solution. AASHTO PP-84-19 has recommended that values of the formation factor be measured at an age of 91 days.

#### 4.3 Sample Conditioning—Temperature Correction

It is vital to correct resistivity measurements for temperature if they are not performed at the standard temperature 23 ± 1°C. The effect of temperature on resistivity measurements on cementitious materials has been described in prior work and several different corrections have been proposed; however, it has been determined that the activation energy of conduction (Arrhenius) type of approach is a fundamental and an accurate representation of the effects of temperature on concrete (Coyle et al., 2018). Equation 4.3 shows the relationship of a resistivity measured at a reference temperature and the resistivity measured at a second temperature.

$$\rho_{T-ref} = \rho_T \exp \left[ \frac{-E_{a-Cond}}{R} \left( \frac{1}{T+273} - \frac{1}{T_{Ref}+273} \right) \right] \quad (\text{Eq. 4.3})$$

Where  $\rho_T$  is the resistivity measured at the testing temperature (Ωm),  $\rho_{Tref}$  is the resistivity of concrete measured at the reference temperature (Ωm),  $T$  is the testing temperature (°C),  $T_{ref}$  is the reference temperature (typically 23°C in the U.S.) (°C),  $E_{a-Cond}$  is the activation energy of conduction (typically 15.8 kJ/mol) (kJ/mol) (Qiao & Coyle et al., 2018), and  $R$  is the universal gas constant, (8.314 J/(mol K)). This correction is illustrated in Figure 4.1 Here it can be seen that when the testing temperature is 10°C the resistivity is

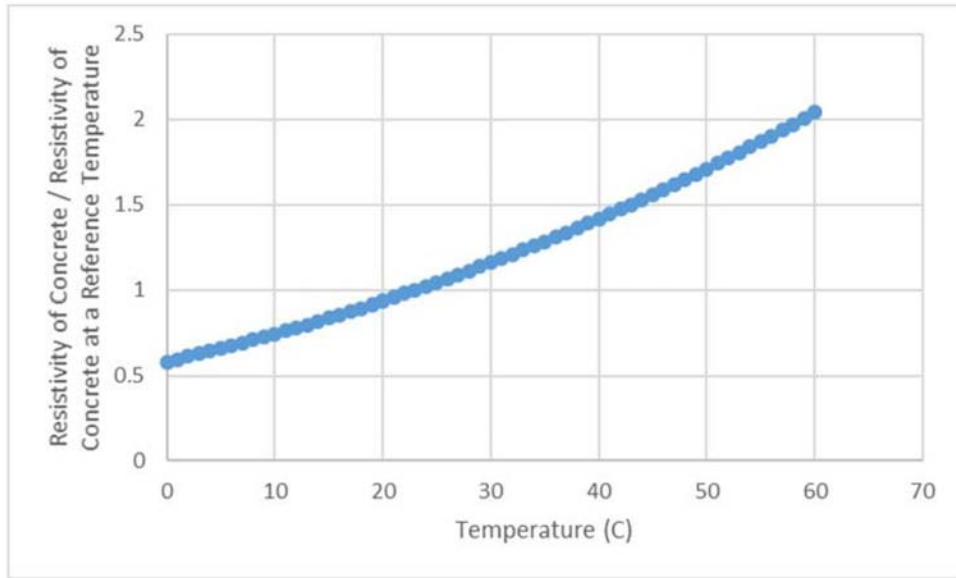


**Figure 4.1** Ratio of the resistivity of concrete at an arbitrary temperature and the resistivity measured at a standard temperature (23°C) based on equation 4.3.

46% of the value at the standard reference temperature and when the testing temperature is 30°C the resistivity is 146% of the value at the standard reference temperature.

#### 4.4 Sample Conditioning—Maturity or Aging

As concrete hydrates (the reaction that occurs as its age increases) the porosity decreases and the resistivity and formation factor generally increase. While the age of the specimen is generally standard laboratory temperature 23 +/- 1°C, samples cured at a higher temperature hydrate faster and have a resistivity that increases faster than samples cured at a lower temperature.

The influence of temperature on the extent of hydration has been described in prior work using a maturity-based approach. Here an activation energy-based approach is used (Arrhenius). Equation 4.4 shows the relationship between the resistivity measured at a reference temperature (i.e., the resistivity measured at x days at 23°C) and the resistivity of the concrete that

is measured when the concrete is maintained at another temperature T.

$$\rho_{Age-ref} = \rho_{Age} \exp \left[ \frac{-E_{a-Hyd}}{R} \left( \frac{1}{T+273} - \frac{1}{T_{Ref}+273} \right) \right] \quad (\text{Eq. 4.4})$$

where  $\rho_{Age}$  and  $\rho_{Age-ref}$  are the resistivities of concrete sample and concrete at a reference temperature respectively, ( $\Omega m$ ), T is the testing temperature and  $T_{ref}$  is the reference temperature (typically 23°C in the U.S.) (°C),  $E_{a-hydration}$  is the activation energy of hydration (typically 41.5 kJ/mol, (Krishnan et al., 2006) (kJ/mol), and R is the universal gas constant, (8.314 J/ (mol K)). Samples stored at a higher temperature hydrate faster than samples stored at a lower temperature. Figure 4.2 shows that samples at 36°C develop resistivity at approximately twice the rate of samples at 23°C. This relationship will be utilized later in this report when the accelerated aging test is developed.

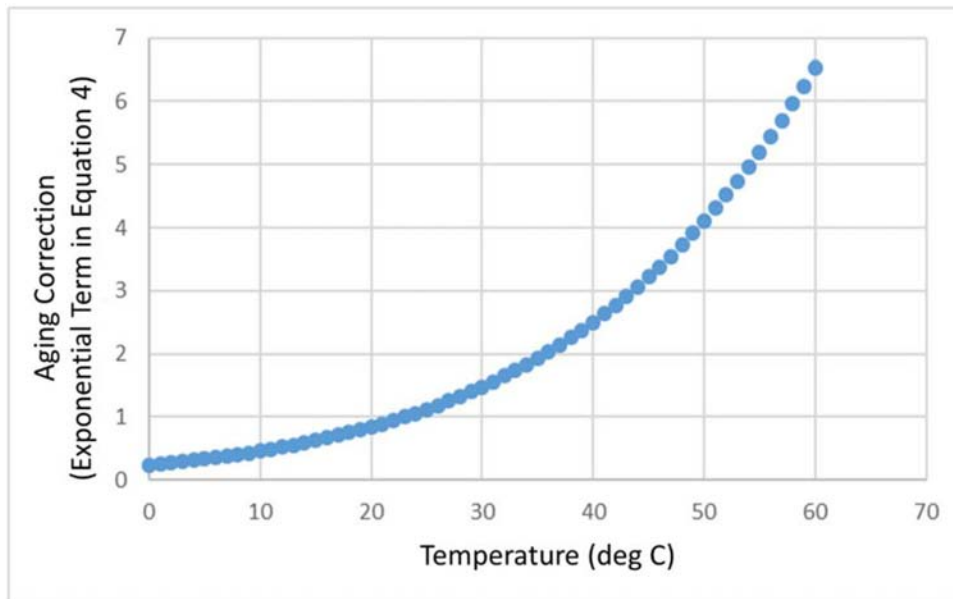
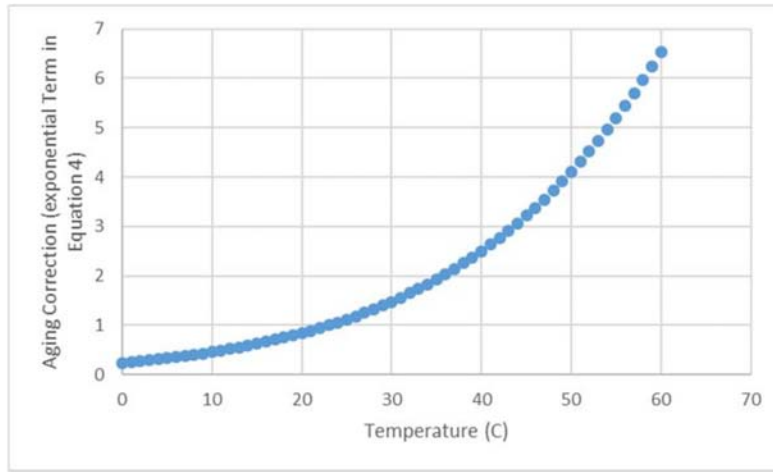


**Figure 4.2** Correction for hydration at different temperatures based on Equation 4.4.

## 5. REVIEW OF MEASURED RESISTIVITY AND FORMATION FACTORS

Eighteen concrete cores from Indiana pavements were received. The mixture proportions from these cores are listed in Table 5.1. They can be separated into six groups according to the mixture proportions.

### 5.1 Porosity

Porosity measurement was conducted on the cylindrical cores with a thickness of  $51 \pm 1$  mm ( $2 \pm 0.04$  in). The volume of permeable pores was determined according to ASTM C642-13 with the exception that the concrete specimens were saturated by vacuum, instead of being placed into boiling water. Vacuum saturation has been shown to be a comparable method of sample conditioning which enables to saturate all air voids in the specimen (Bu et al., 2014). After the specimens were oven dried at  $105 \pm 2^\circ\text{C}$  ( $212 \pm 3.6^\circ\text{F}$ ), the mass was measured and then they were placed into the vacuum chamber with a vacuum level of  $933 \pm 266$  Pa ( $7 \pm 2$  Torr) for three hours. Alkali solution (NaOH + KOH mixture solution, with a resistivity of  $0.04 \Omega\cdot\text{m}$ ) was drawn into the vacuum chamber and specimens were maintained in vacuum for another hour. The specimens were kept submerged for another 20 hours after the vacuum session. The mass of the surface-dry samples and their apparent mass under water were measured to calculate the porosity.

The measured porosity of the concrete pavement cores lies in the range of 18%–25%, depending on the different amounts of cementitious materials. Figure 5.1 provides a plot of the measured porosity as a function of the paste volume. As the paste volume increases the porosity increases. It should also be noted that variations in the air content can also impact the measured porosity.

### 5.2 Electrical Resistivity

The electrical resistivity and formation factor of saturated concrete were measured on the vacuum saturated concrete specimen after the porosity measurement. The cores were kept submerged in the solution for two weeks prior to measurements to enable the samples to reach equilibrium. The resistance of the specimens was measured using a Giatec RCON2™ resistivity meter with a frequency of 1 kHz at  $23 \pm 1^\circ\text{C}$ . Two 102-mm diameter stainless steel plate electrodes were used with two pieces of sponge with a thickness of 3 mm. During the test, the sponge was saturated with lime water and placed between specimens and plate electrodes to ensure the electrical connection. The electrical resistivity was calculated using the measured electrical

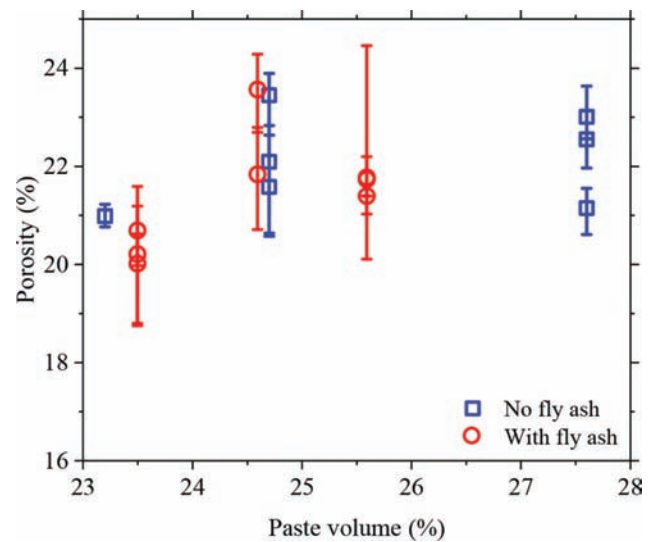


Figure 5.1 Porosity of concrete pavement cores.

TABLE 5.1  
The Mixture Proportion of the Concrete Cores (lb/yd<sup>3</sup>)

Core NO.	INDOT CMD NO.	Coarse Aggregates	Fine Aggregate	Cement	Fly Ash	Water	Air Content <sup>a</sup> (%)	w/cm	Fly Ash Level by Volume	Paste Volume Portion (%)
1, 2, 3	113501017	1693	1277	564	~	237	6.5	0.42	~	24.7
4, 7, 8, 13	123501004	1664	1251	480	106	237.5	6.5	0.41	0.21	25.6
5, 6, 9	123501017	1615	1215	630	~	264.5	6.5	0.42	~	27.6
10, 11, 12	133501005	1777	1375	400	125	220.5	6.5	0.42	0.28	23.5
14, 17, 18	133501010	1719	1297	530	~	222.5	6.5	0.42	~	23.2
15, 16	133501992	1685	1271	452	112	228.5	6.5	0.41	0.23	24.6

<sup>a</sup>Air is based on the values reported when samples were received.

Note: Four experiments were performed on the concrete pavement cores, including the porosity, electrical resistivity, thermogravimetric analysis, and low temperature differential scanning calorimetry. The results of these tests are described in the following sections.

resistance minus the resistance of two pieces of sponge as described in AASHTO TP-119-19 (Option C).

Figure 5.2 shows the electrical resistivity of the cored concrete pavements.

Figure 5.3 shows the formation factor (F) of the cored concrete pavements calculated from Equation 5.1:

$$F = \frac{\rho_{SAT}}{\rho_{ps-SAT}} = \frac{1}{\phi \cdot \beta} \quad (\text{Eq. 5.1})$$

where,  $\rho_{SAT}$  is the electrical resistivity of the concrete pavement ( $\Omega \cdot m$ ),  $\rho_{ps-SAT}$  is the electrical resistivity ( $\Omega \cdot m$ ) of the pore solution,  $\phi$  is the porosity, and  $\beta$  is the connectivity of the pore network. The value of  $\rho_{ps-SAT}$  is the same as the resistivity of the simulated pore solution that was used in this investigation (0.04  $\Omega \cdot m$ ). It should be noted that this testing was done prior to standardization on the value of 0.127  $\Omega \cdot m$ . While the

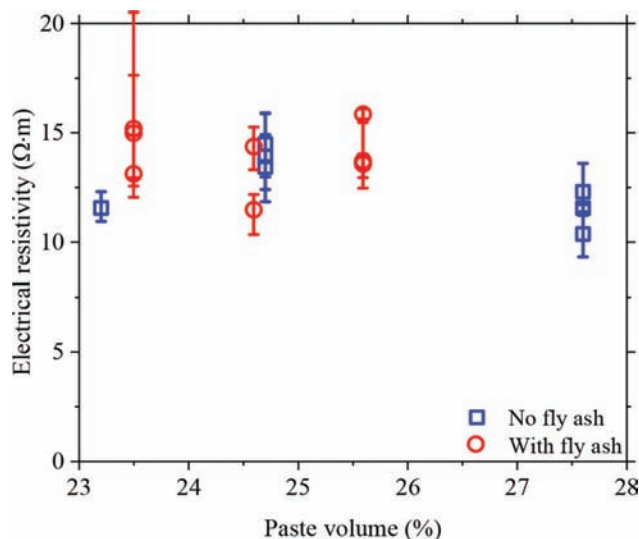


Figure 5.2 Electrical resistivity of concrete pavement cores.

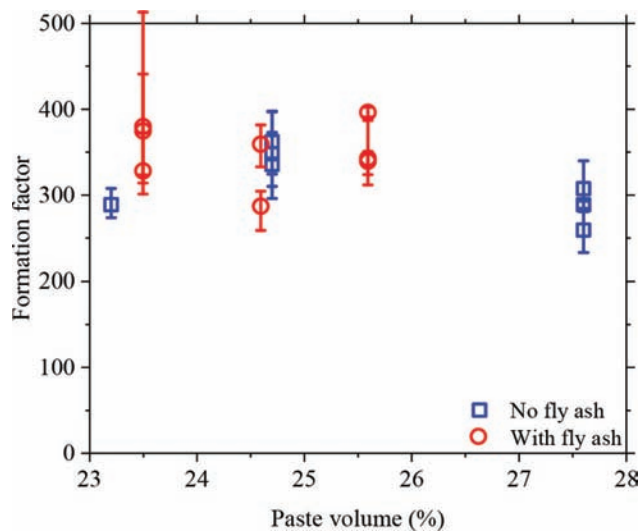


Figure 5.3 Formation factor of concrete pavement cores.

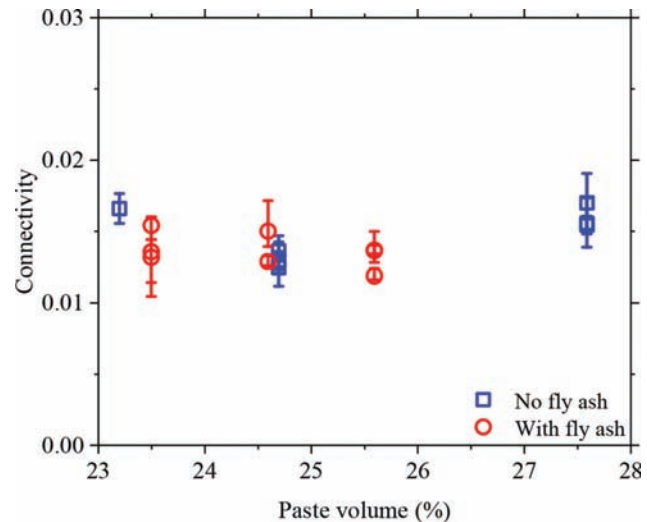


Figure 5.4 Pore network connectivity of concrete pavement cores.

resistivity of the pore solution impacts the values of resistivity measured it does not impact the formation factor. As such the formation factor will be used in the remainder of the report.

The connectivity of the pore network of the concrete can be calculated using Equation 4.3 and the measured properties. The connectivity is shown in Figure 5.4 demonstrates that at higher paste volumes both the porosity and connectivity are elevated. The higher pore volume in a concrete with a higher paste results in a larger number of flow paths and a higher connectivity. At low porosity values the connectivity may also be elevated presumably due to either a lack of consolidation or/and the connectivity of interfacial transition zones. As such, it appears that there may be an optimal value of paste for a given aggregate grading that can result in a minimized connectivity and formation factor. This should be considered when mixtures are being developed to with lower binder contents. First, for lower binder content mixtures aggregate gradation and packing is important. Several methods exist to optimize the aggregate gradation. Second, while lower paste contents are beneficial, it appears that the paste content can be reduced to a value that increases transport. More research is needed to determine the exact gradations and paste contents that this would occur at for INDOT materials.

### 5.3 Thermogravimetric Analysis (TGA)

TGA was performed on the ground concretes to determine the amount of  $\text{Ca}(\text{OH})_2$ . The test was performed by placing approximately 30 mg of ground material (concrete) in a platinum pan, which was heated to 500°C at a rate of 10°C/min in an inert nitrogen atmosphere. The  $\text{Ca}(\text{OH})_2$  content was determined based on the mass loss between approximately 380°C and 460°C. The  $\text{Ca}(\text{OH})_2$  amounts are presented here as g/100 g powder, where powder refers to the original mass of the ground concrete sample.

#### 5.4 Low Temperature Differential Scanning Calorimetry (LT-DSC)

LT-DSC was used to determine the amount of CAOXY produced due to the reaction of the  $\text{Ca(OH)}_2$  in the cementitious materials with  $\text{CaCl}_2$  solutions. This was done using AASHTO T-365-17 (a procedure based on earlier INDOT studies (Monical et al., 2016)). Ground concrete powder was mixed with 20%  $\text{CaCl}_2$  solution at varying powder-liquid ratio, ranging from one to seven. The reasoning for studying different ratios in concretes as compared to pastes is that the 1:1 ratio selected for pastes was based on  $\text{Ca(OH)}_2$  proportions in the paste, which are quite different from the  $\text{Ca(OH)}_2$  proportions in concretes because of the dilution caused by the aggregates. For these concrete samples, the powder mass ranged from  $10 \pm 0.5$  mg to  $28 \pm 0.5$  mg and the solution mass ranged from  $2.5 \pm 0.5$  mg to  $10 \pm 0.5$  mg.

After the pan was sealed, it was then placed in the LT-DSC and subjected to the following temperature cycle: isothermal at  $25^\circ\text{C}$  for 60 minutes; followed by cooling  $3^\circ\text{C}/\text{min}$  until  $-90^\circ\text{C}$ ; followed by a low temperature loop from  $-90^\circ\text{C}$  to  $-70^\circ\text{C}$  to  $-90^\circ\text{C}$ , at a rate of

$3^\circ\text{C}/\text{min}$ ; followed by heating to  $50^\circ\text{C}$  at a rate of  $0.25^\circ\text{C}/\text{min}$ . At approximately  $30^\circ\text{C}$ , the CAOXY undergoes a phase transition that can be detected. The latent heat associated with the CAOXY phase transition can be measured between the two temperature steps of the transition, and by comparing the latent heat with that measured for pure CAOXY (186 J/g), the amount of CAOXY formed in a mixture can be found. Under these conditions, cement paste samples had a coefficient of variation of approximately 5%. Unless otherwise specified, CAOXY amounts are presented here as g/100 g powder, where powder refers to the original mass of the ground concrete sample.

Figure 5.5 shows the relationship between the measured  $\text{Ca(OH)}_2$  content and amount of calcium oxychloride (CAOXY). As the  $\text{Ca(OH)}_2$  content increases, the amount of CAOXY increase. When the  $\text{Ca(OH)}_2$  content is below about 1% w.t, there is no calcium oxychloride formed, which may indicate that the external  $\text{CaCl}_2$  solution has little access to the small amount of  $\text{Ca(OH)}_2$  encapsulated by other hydration products. Another hypothesis is that the  $\text{Ca(OH)}_2$  is consumed due to the pH drop of the system during the exposure.

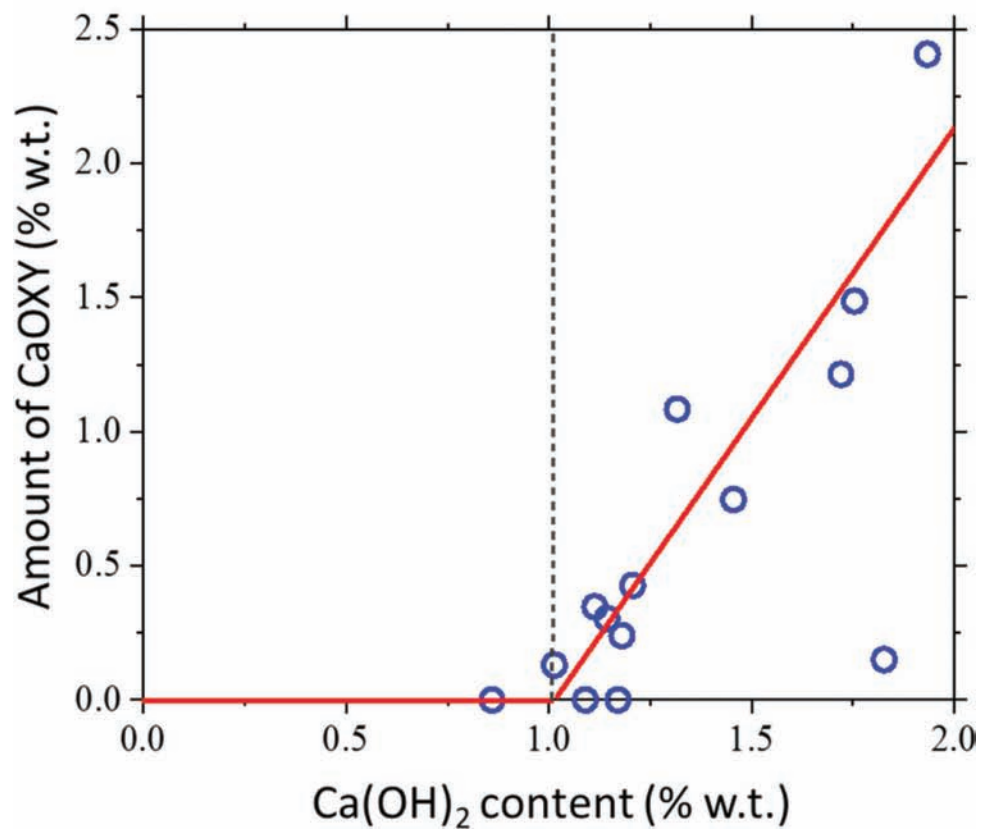
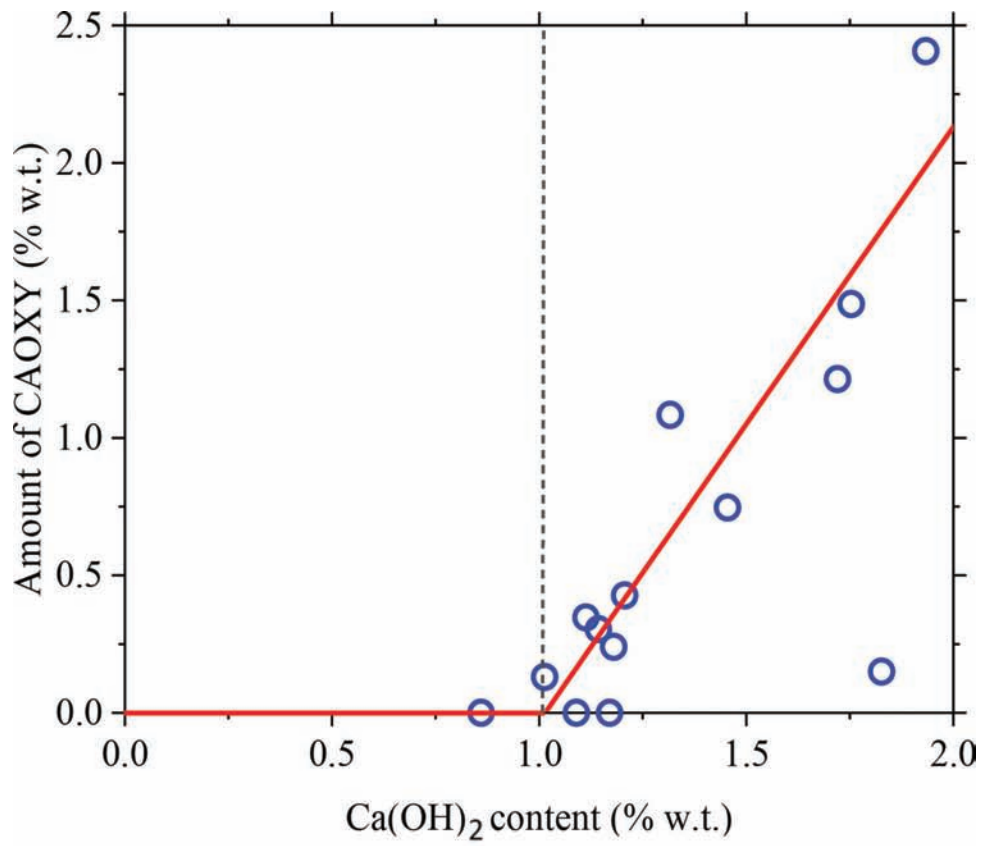


Figure 5.5 Relationship between the Ca(OH)<sub>2</sub> content and the amount of formed CAOXY.

## 6. ESTABLISH TESTING TIMES FOR THE ACCELERATED TESTING PROCEDURES

One goal of this research was to establish testing times and/or an acceptable accelerated aging procedure for use in acceptance testing. The AASHTO subcommittee on materials suggested to the PI in a national study that 91-day ages would be the most beneficial for assessing the transport properties of concrete to enable supplementary materials to be evaluated fairly. As such this was incorporated in AASHTO PP-84. It should also be noted that unpublished work by the PI has shown that frequently little benefit is achieved in improving the overall transport properties after approximately 120 days in transportation systems. Presumably this is due to slow reaction rates and limited water in practice. As such, the goal of this research was to develop a method to attain an equivalent age of 91 days at an actual age of 28 days.

Toward this end, the research team has proposed a temperature profile for testing that is shown in Figure 6.1. The samples would be maintained at 23 +/- 2°C for 3 days. This early conditioning is done to allow the microstructure to initially develop at a standard temperature 23 +/- 2°C. After these 3 days the sample temperature is elevated to 50 +/- 3°C and held at this temperature until an actual age of 28 days. At an actual age of 28 days the temperature is returned to room temperature to measure the sample at 23 +/- 2°C to enable the resistivity to be measured.

This temperature history was established using a maturity-based approach as outlined in Equation 4.4. In an earlier study the activation energy for hydration was found to vary for materials/mixtures used by

INDOT from approximately 30 to 52 kJ/mol with a typical value of 41.5 kJ/mol (Coyle et al., 2018; Krishnan et al., 2006; Qiao et al., 2018; Sant et al., 2008). Based on these results activation energies were used with two standard deviations from the average were used along with Equation 4.4 to develop Figure 6.2. It can be seen that the lower bound of samples achieves nearly 90 days of hydration while the upper bound achieves an equivalent age of 120 days.

Bu et al. (2014) demonstrated that heating the samples could be used provided that care was taken to not oversaturate the samples during heating and cooling.

While laboratories often place the samples (and the 5-gallon bucket they are stored in) in an oven or fluid bath to achieve temperature, other approaches may be needed for use in the field. It is recommended that the use of insulated pail heaters (for 5-gallon buckets) be considered. These pail heaters can be purchased relatively inexpensively and may work well for this application.

It should be noted that another popular method of accelerated curing is to subject specimens to 7 days of standard curing followed by 21 days of curing in lime-saturated water at 100°F (38°C). This accelerated procedure is described in ASTM C1202 (Obla et al., 2016; Ozyildirim, 1998). The temperature profile is outlined in Figure 6.3 while Figure 6.4 provides an indication of the equivalent age of concrete achieved by this method. Unlike the proposed method which achieves a 91-day equivalent for each of the activation energies used, this method achieves equivalent ages of between 51 and 62 days at the end of testing.

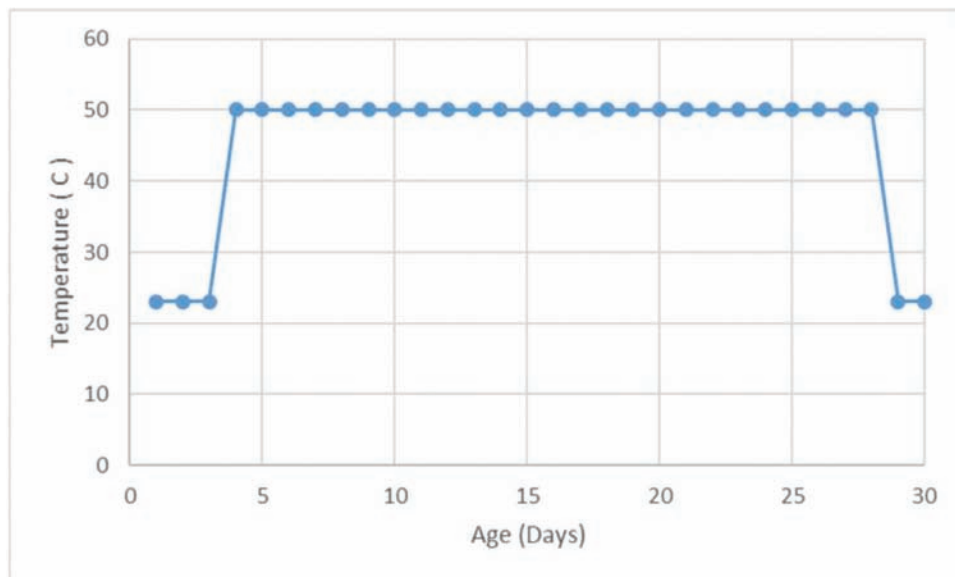


Figure 6.1 Temperature profile of the accelerated curing condition.



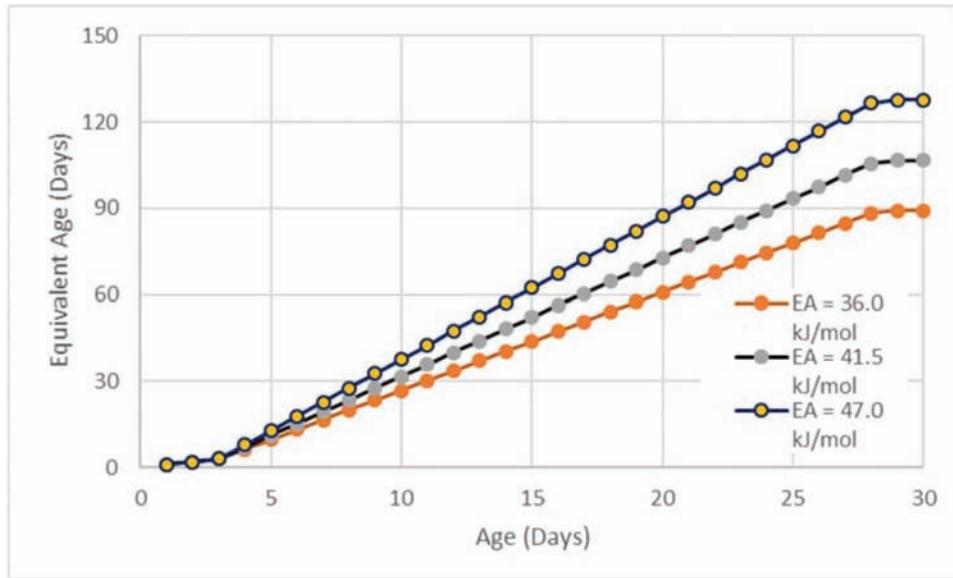


Figure 6.2 Equivalent age as a function of activation energy.

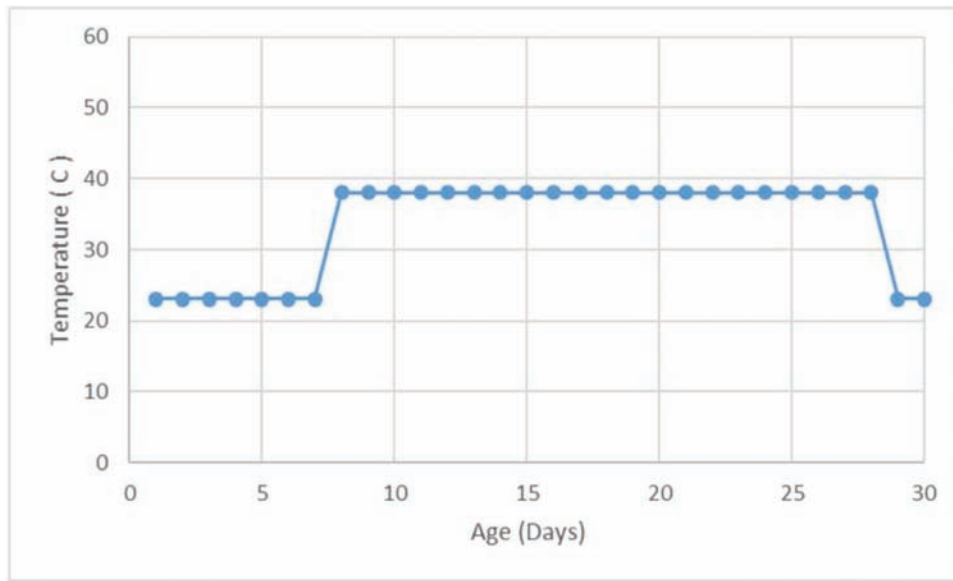
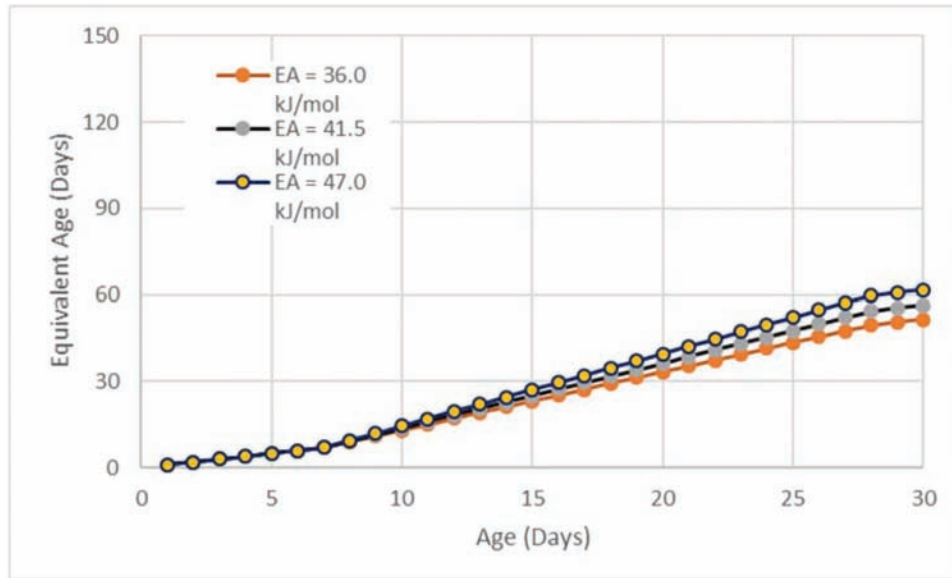


Figure 6.3 Temperature profile of the accelerated curing condition in ASTM C1202.



**Figure 6.4** Equivalent age as a function of activation energy using the accelerated curing procedure in ASTM C 1202.

As a result, it is recommended that the accelerated curing consist of 3 days at 23 +/- 2°C, followed by curing at 50 +/- 3°C until an actual age of 28 days after which time the temperature is reduced to 23 +/- 2°C for at least 12 hours.

## 7. ESTABLISHED FORMATION FACTORS FOR PAVEMENTS

In the preliminary development of this research program it was anticipated that there would be a need to develop a procedure and worksheet that can be used to convert the formation factor to a job specific resistivity that can be used during the job mixture specification process. This was originally anticipated since it was expected that the pore solution that was “matched” to each concrete composition. As such, the simulated pore solution would have been dependent on the job mix formula. However, as the research team discussed this the SAC and other members of state highway organizations across the U.S. a simplified procedure was developed where the pore solution has been standardized for all mixtures (i.e., AASHTO TP-119-19 Option A). This compromise (to utilize a standard pore solution as described in AASHTO TP-119-19 Option A) was arrived at as a simplification to avoid potential errors in the field in pore solution preparation. As a result, Table 7.1 can provide a direct calculation that relates the formation factor to the resistivity assuming a pore solution resistivity of 0.127 Ωm for saturated concrete. These results are also compared to the classification provided in AASHTO T277 for a point of reference.

It should however be noted that Table 5.1 refers to saturated concrete. Samples conditioned in accordance with AASHTO TP-119-19 Option A will not be fully saturated and will be in a state where the gel and capillary voids are fluid filled however the air voids

remain empty (this is referred to as matrix saturation). As a result, the apparent formation factor needs to be introduced to account for the partial saturation provided by AASHTO TP-119-19 Option A. An empirical relationship has been developed (Qiao & Moradillo et al., 2018) to relate the saturated formation factor to an apparent formation factor (a formation factor that varies as a function of the degree of saturation as shown in Figure 7.1. Using this approach and recognizing that a typical concrete paving mixture for INDOT will have a matrix saturation of approximately 70% Table 7.2 was developed.

AASHTO PP-84 states that, “Concrete not subjected to freezing and thawing or deicer application: apparent formation factor F greater than 500 and Concrete subjected to freezing and thawing and deicer application: apparent formation factor F greater than or equal to 1000.”

It should be noted that AASHTO PP-84-19 is currently recommending that paving mixtures have an apparent formation factor of 1,000 when deicing salts may be applied which corresponds to an apparent resistivity of 12.7 kΩ cm (127 Ω m). This corresponds to a saturated formation factor of approximately 343 (saturated resistivity of 4.4 kΩ cm (44 Ω m). This can be compared with the values in Figure 5.3 where INDOT mixtures were found to have a Saturated Formation Factor of approximately 260–400. While the INDOT mixtures are in the vicinity of this limit and many achieve this value, they are not all above this limit. Some common ways to improve the formation factor are the use of reactive supplementary materials, the reduction of water to cement ratio, and the optimal use of paste content. Mixture with too high or too low a paste volume tends to have lower formation factors. As a result, it is recommended that INDOT monitor this with current mixture designs before any specification changes that would be implemented.

TABLE 7.1  
Relationship Between Results of the RCPT Test, the Saturated Formation Factor, and the Saturated Resistivity

Chloride Ion Penetrability	Minimum Charge Passed @ 6 hrs <sup>a</sup> Coulombs	Minimum Charge Passed @ 6 hrs <sup>a</sup> Coulombs	Saturated Formation Factor <sup>b</sup> ~	Saturated Formation Factor <sup>b</sup> ~	Saturated Resistivity <sup>c</sup> kΩ cm	Saturated Resistivity <sup>c</sup> kΩ cm	Saturated Resistivity <sup>c</sup> Ω m	Saturated Resistivity <sup>c</sup> Ω m
High	4000	~	407	~	5.2	~	52	~
Moderate	2000	4000	814	407	10.3	5.2	103	52
Low	1000	2000	1629	814	20.07	10.3	207	103
Very Low	100	1000	16286	1629	207.0	20.7	2070	207
Negligible	0	100	~	16286	~	207.0	~	2070

<sup>a</sup>As determined from T 277.

<sup>b</sup>A conversion between the F<sub>APP</sub> value and RCPT (T 277) and resistivity (T 358) is provided assuming a pore solution resistivity of 0.127 Ω·cm.

<sup>c</sup>As determined based on first principles (Spragg et al., 2013) using T 358 or TP 119, assuming a saturated sample.

TABLE 7.2  
Relationship Between Results of the RCPT Test, the Apparent Formation Factor, and the Apparent Resistivity (Degree of Saturation Has Been Assumed to Be 70%)

Chloride Ion Penetrability	Minimum Charge Passed @ 6 hrs <sup>a</sup> Coulombs	Minimum Charge Passed @ 6 hrs <sup>a</sup> Coulombs	Apparent Formation Factor <sup>b</sup> ~	Apparent Formation Factor <sup>b</sup> ~	Apparent Resistivity <sup>c</sup> kΩ cm	Apparent Resistivity <sup>c</sup> kΩ cm	Apparent Resistivity <sup>c</sup> Ω m	Apparent Resistivity <sup>c</sup> Ω m
High	4000	~	1187	~	15	~	151	~
Moderate	2000	4000	2374	1187	30	15	302	151
Low	1000	2000	4748	2374	60	30	603	302
Very Low	100	1000	47481	4748	207	60	2070	603
Negligible	0	100	~	47481	~	207	~	2070

<sup>a</sup>As determined from T 277.

<sup>b</sup>A conversion between the F<sub>APP</sub> value and RCPT (T 277) and resistivity (T 358) is provided assuming a pore solution resistivity of 0.127 Ω·cm. This also assumes a matrix saturation of 70%.

<sup>c</sup>As determined based on first principles, then applying a saturation function with a DOS of 70%.

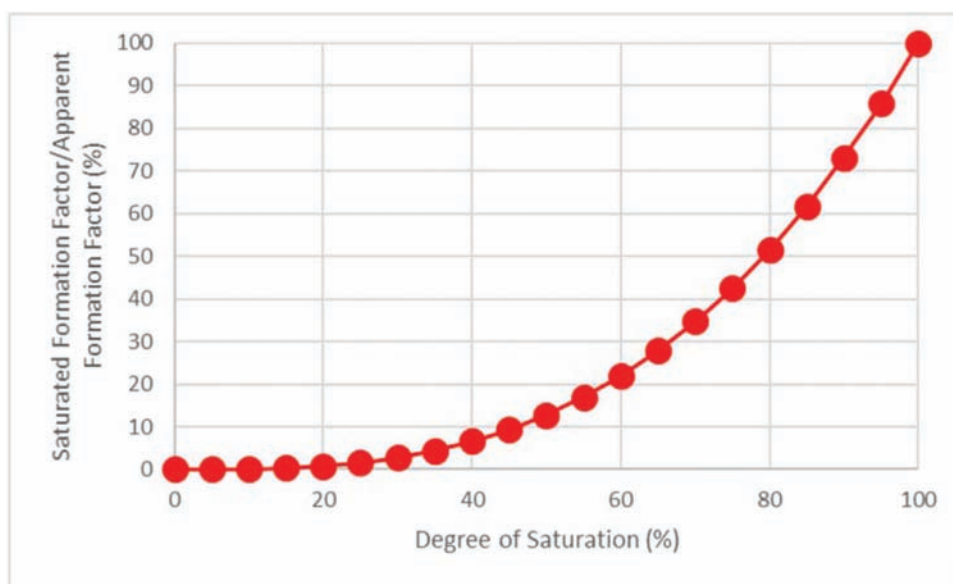


Figure 7.1 The ratio of the formation factor and apparent formation factor as a function of the degree of saturation.

It is also recommended that to account for construction variation (a COV of approximately 10%) that the trial batches have a target that greater than the acceptance specification. Assuming a one-sided distribution with 90% confidence it is recommended that the resistivity targeted for the trial batch is 1.16 times that of the acceptance value for resistivity. To comply with AASHTO PP-84-16 recommendations it would be recommended that the trial batch target a value of 14.8 kΩ cm while the acceptance value during construction would be 12.7 kΩ cm.

## 8. ESTABLISHED FORMATION FACTORS FOR OTHER ELEMENTS

While Section 7.0 correlated formation factor and resistivity to AASHTO PP-84-16 for pavements, there are times where the formation factor may be related to service life for other elements like a bridge deck. The use of the formation factor has advantages as compared to more commonly used approaches such as specifying a value of the diffusion coefficient measured by ponding or impressed current since the formation factor can be used in quality control procedures due to its relative ease of testing.

Toward this end the Nernst-Plank modeling approach can be used to relate the formation factor (along with porosity and chloride binding) directly to predict chloride ingress as a function of time and service life (Isgor & Weiss, 2019; Qiao & Coyle et al., 2018). This is the method recommended by the authors as it is the more accurate of the two methods. Full details on this approach are provided in (Isgor & Weiss, 2019).

However, often the end user would like to relate the formation factor to a diffusion coefficient. It is however important to make a distinction between an effective

diffusion coefficient ( $D_{EFF}$ ) and an apparent diffusion coefficient ( $D_{APP}$ ).  $D_{EFF}$  does not consider binding and can be related to the formation factor using Equation 8.1:

$$D_{EFF} = \frac{D_o}{F} \quad (\text{Eq. 8.1})$$

where  $D_o$  is the self-diffusion coefficient of an ion (here a chloride ion) in infinitely diluted bulk solution.

A one-dimensional diffusion process can be described using Equation 8.2 with Cranks solution of Fick's second law where the traditional  $D$  (diffusion coefficient) has been replaced with  $D_o/F$ , from the Nernst-Einstein relationship (Spragg & Weiss, 2016; Weiss et al., 2016; Weiss et al., 2017):

$$\frac{C_x - C_o}{C_s - C_o} = 1 - \text{erf} \left[ \frac{x}{2\sqrt{\left(\frac{D_o}{F}\right)t}} \right] \quad (\text{Eq. 8.2})$$

where  $C_s$  is the surface salt concentration,  $C_o$  is the original chloride concentration,  $C_x$  is the chloride concentration at the depth of  $x$  at time  $t$  and  $D_o$  is the self-diffusion coefficient for a chloride ion ( $2.03 \times 10^{-9} \text{ m}^2/\text{s}$  at  $25^\circ\text{C}$ ). When  $C_x$  exceeds the chloride threshold at time  $t$ , depassivation occurs and corrosion is assumed to initialize.

Figure 8.1a illustrates the relationship between the formation factor and the time to corrosion repair for concrete elements with differing cover thicknesses (assuming surface concentration ( $C_s$ ) of 0.7% of the mass of concrete, a chloride threshold ( $C_x$ ) of 0.15% of the mass of concrete considering a corrosion inhibitor was used, and an initial chloride concentration ( $C_o$ ) of 0% of the mass of concrete). Figure 8.1b shows the time to

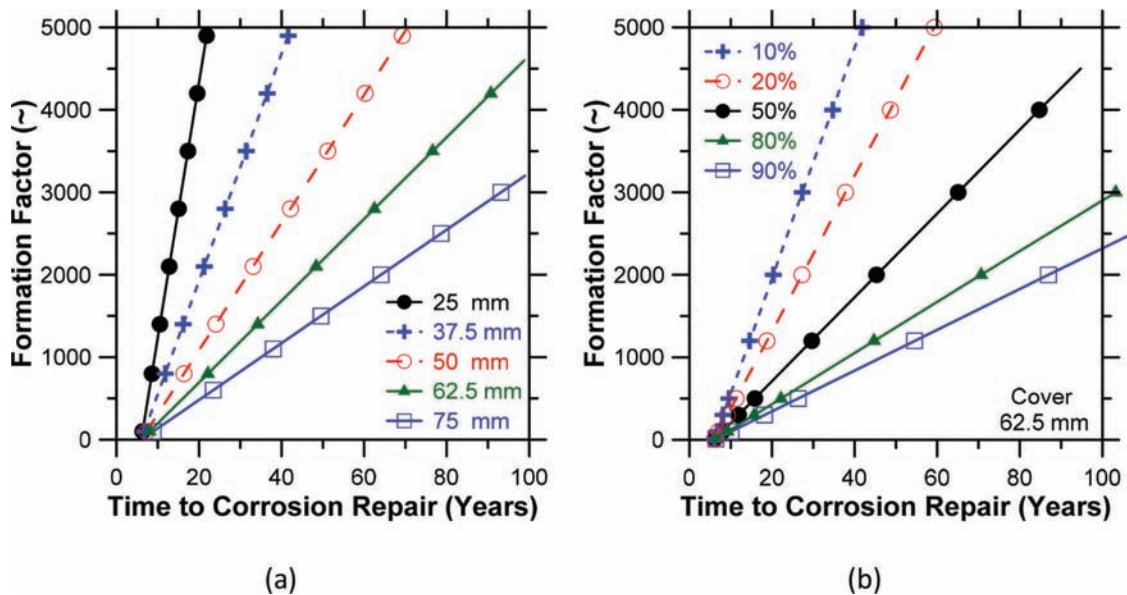


**Figure 8.1** Predicted time to corrosion: (a) influence of cover thickness (b) variability in the percentage of elements requiring repair.

corrosion repair with different levels of damage serving as the trigger for repair, i.e., 10% represents a case where repair is done when 10% of elements are needing repair. Figure 8.1a illustrates that a formation factor of 1,200 or greater would be needed to provide a concrete element with a 62.5 mm cover with a life of 30 years (24 years to depassivation plus 6 years of propagation). As mentioned, this approach considers no chloride binding.

Since the aforementioned approach does not include chloride binding many in the concrete community prefer to use  $D_{APP}$  with Fick's second law. Toward this end Azad et al. (2018) developed a procedure where  $D_{APP}$  can be estimated using a chloride binding isotherm, porosity, and the formation factor. This procedure is described in detail in (Azad et al., 2018) and a short summary is included here. To begin the chloride binding isotherm ( $C_B$ ) will be assumed to have a Freundlich form as shown in Equation 8.3:

$$C_B = \alpha C_f^\beta \quad (\text{Eq. 8.3})$$

where  $C_F$  is the free chloride concentration,  $\alpha$  and  $\beta$  are fitting parameters. To obtain the fitting parameters experimentally 10 g of ground concrete powder is mixed with 10 mL NaCl solution with different initial concentrations (for example concentrations of 100; 300; 500; 1,000; 1,500; 2,000; and 3,000 mol/m<sup>3</sup> have been used) and stored for 7 days at  $23 \pm 1^\circ\text{C}$ . After 7 days of exposure, the concentrations of equilibrated solutions were determined, the bound chloride content and Equation 8.3 is fitted to the data (full details are provided in Azad et al., 2018). Values of  $\alpha$  measured for a series of concretes were between 0.4 and 1.5 while values for  $\beta$  ranged between 0.16 and 0.53.

$D_{APP}$  can then be computed using Equation 8.4:

$$D_{App} = \frac{D_o}{\phi F \left( 1 + \frac{1.25}{\phi} \alpha \beta C_{exp}^{\beta-1} \right)} \quad (\text{Eq. 8.4})$$

where  $\phi$  is the porosity and  $C_{exp}$  is the concentration of the salt solution at the exposed surface? It should be noted that an AASHTO procedure has recently been developed for determining the porosity of concrete. It is recommended that a standard for chloride binding is also developed as either an ITM or an AASHTO standard.

The surface chloride concentration,  $C_{s-app}$ , can be obtained using Equation 8.5.

$$C_{S-app} = \phi C_{exp} - \alpha C_{exp}^\beta \quad (\text{Eq. 8.5})$$

Using the values from Equations 8.4 and 8.5, Cranks solution for Fick's second law (Equation 8.4) can be used to compute the time required for chloride ions to reach a critical level at the surface of the reinforcing steel.

$$\frac{C_x - C_o}{C_{s-app} - C_o} = 1 - \text{erf} \left[ \frac{x}{2\sqrt{(D_{APP})t}} \right] \quad (\text{Eq. 8.6})$$

## 9. REPORTING ACCELERATED TESTING PROCEDURES

As AASHTO TP-119-19—Option A has been standardized and is being widely adopted across the country by state highway agencies (SHA's) there is no need for a pore solution computation for each concrete composition. This greatly simplifies field testing and testing during the trial batch.

It is important to note that the temperature of the test specimen at the time of testing can significantly influence the measurements of electrical resistivity. An increase in the temperature of the specimen results in a decrease in the resistivity. A decrease in the temperature of the specimen results in an increase in resistivity. Specimens shall always be tested and conditioned at standard temperatures, i.e.,  $23 \pm 2^\circ\text{C}$ .

It is recommended that AASHTO TP-119-19 Option A be used by INDOT for trial batches and quality assurance or quality control testing.

The current testing and reporting requirements of AASHTO TP-119-19 include a curing history of the sample, which could be performed as either of the following:

- Standard curing where the sample is placed in the pore solution at the time of demolding (1 day) and maintained at  $23 \pm 2^\circ\text{C}$  for the duration of the test, typically 91 days.
- Accelerated curing where the sample is placed in curing solution at the time of demolding where it is maintained at  $23 \pm 2^\circ\text{C}$ . At an age of 3 days the temperature of the sample is increased to  $50 \pm 3^\circ\text{C}$  until an actual age of 28 days after which time the temperature is reduced to  $23 \pm 2^\circ\text{C}$  for at least 12 hours.

It is currently recommended that when the accelerated curing conditions are used this is clearly noted. This could include a simple statement that "Testing was performed in accordance with Option A of AASHTO TP-119-19 where accelerated curing was used. Accelerated curing consisted of maintain the specimens at  $23.0 \pm 2.0^\circ\text{C}$  for 3 days before the samples were heated to  $50.0 \pm 3.0^\circ\text{C}$ . The samples were returned to  $23.0 \pm 2.0^\circ\text{C}$  for a minimum of 12 hours before testing."

## 10. SUMMARY OF FINDINGS

Resistivity can be measured using AASHTO TP-119-19. Option A is currently recommended for its simplicity.

- Samples were tested to establish the current levels of performance for concrete pavements in the state of Indiana. INDOT mixtures were found to have a Saturated Formation Factor of approximately 260–400.
- The role of sample conditioning indicates that by submerging samples in a simulated pore solution enables the matrix saturation to be reached. This measures transport through the matrix. This implies that apparent formation factor and apparent resistivity should be used to describe the results.

- Field samples were tested and may indicate that high paste contents can have a greater connectivity due to the increased porosity of the concrete. It is also noted that concrete with a very low paste content can have an increase in connectivity, presumably due to the connection of the interfacial transition zones and potentially insufficient consolidation.
- Accelerated curing consisted of maintain the specimens at 23.0 +/- 2.0°C for 3 days before the samples were heated to 50.0 +/- 3.0°C. The samples were returned to 23.0 +/- 2.0°C for a minimum of 12 hours before testing. The use of this procedure enables the reactions of supplementary materials to be more fully considered.
- A methodology is reviewed whereby the formation factor can be related to either typical formation factor or resistivity values based on AASHTO PP-84 or where the formation factor can be used to determine either an effective or apparent diffusion coefficient to predict service life.

## REFERENCES

- Azad, V. J., Erbehtas, A. R., Qiao, C., Isgor, O. B., & Weiss, W. J. (2018). Relating the formation factor and chloride binding parameters to the apparent chloride diffusion coefficient of concrete. *Journal of Materials in Civil Engineering*, 31(2). [https://doi.org/10.1061/\(ASCE\)MT.1943-5533.0002615](https://doi.org/10.1061/(ASCE)MT.1943-5533.0002615)
- Barrett, T. J., Miller, A. E., & Weiss, W. J. (2015). *Documentation of the INDOT experience and construction of the bridge decks containing internal curing in 2013* (Joint Transportation Research Program Publication No. FHWA/IN/JTRP-2015/10). West Lafayette, IN: Purdue University. <https://doi.org/10.5703/1288284315532>
- Bu, Y., Spragg, R., & Weiss, W. (2014). Comparison of the pore volume in concrete as determined using ASTM C642 and vacuum saturation. *Advances in Civil Engineering Materials*, 3(1), 308–315. <https://doi.org/10.1520/ACEM20130090>
- Bu, Y., Spragg, R., Villani, C., & Weiss, J. (2014, September 14). The influence of accelerated curing on the properties used in the prediction of chloride ingress in concrete using a Nernst–Planck approach. *Construction and Building Materials*, 66, 752–759. <https://doi.org/10.1016/j.conbuildmat.2014.04.138>
- Coyle, A., Spragg, R., Suraneni, P., Amirkhani, A., & Weiss, W. J. (2018, April 19). Comparison of linear temperature corrections and activation energy temperature corrections for electrical resistivity measurements of concrete. *Advances in Civil Engineering Materials*, 7(1), 174–187. <https://doi.org/10.1520/ACEM20170135>
- Isgor, O. B., & Weiss, W. J. (2019). A nearly self-sufficient framework for modelling reactive-transport processes in concrete. *Materials and Structures*, 52(3), 3. <https://doi.org/10.1617/s11527-018-1305-x>
- Krishnan, A., Mehta, J. K., Olek, J., & Weiss, W. J. (2006). *Technical issues related to the use of fly ash and slag during late-fall (low temperature) construction season* (Joint Transportation Research Program Publication No. FHWA/IN/JTRP-2005/5). <https://doi.org/10.5703/1288284313382>
- McCarter, W. J., Forde, M. C., & Whittington, H. W. (1981, December). Resistivity characteristics of concrete. In *Proceedings of the Institution of Civil Engineers, Part 2—Design & Construction*, 71(1), 107–111. <https://doi-org.ezproxy.lib.purdue.edu/10.1680/icep.1981.2142>
- Monical, J., Unal, E., Barrett, T., Farnam, Y., & Weiss, W. J. (2016). Reducing joint damage in concrete pavements: Quantifying calcium oxychloride formation. *Transportation Research Record: Journal of the Transportation Research Board*, 2577(1), 17–24. <https://doi.org/10.3141/2577-03>
- Moradillo, M. K., Hall, H., Reese, S., & Weiss, W. J. (2019). Quantifying fluid absorption in air-entrained concrete using neutron radiography. *ACI Materials Journal*, 116(6), 213–226. <https://doi.org/10.14359/51716980>
- Obla, K. H., Lobo, C. L., & Kim, H. (2016). Test and criteria for concrete resistant to chloride ion penetration. *American Concrete Institute Materials Journal*, 113(5), 621–631. <https://doi.org/10.14359/51689107>
- Ozyildirim, C. (1998, February). *Effects of temperature on the development of low permeability in concretes* (VTRC 98-R14). Virginia Transportation Research Council. [http://www.virginiadot.org/vtrc/main/online\\_reports/pdf/98-r14.pdf](http://www.virginiadot.org/vtrc/main/online_reports/pdf/98-r14.pdf)
- Presuel-Moreno, F., Liu, Y., & Paredes, M. (2009). *Concrete resistivity on the apparent surface resistivity measured via the four-point wenner method*. Presented at the Corrosion 2009 Conference & Expo.
- Qiao, C., Coyle, A., Isgor, O. B., & Weiss, W. (2018). Prediction of chloride ingress in saturated concrete using formation factor and chloride binding isotherm. *Advances in Civil Engineering Materials*, 7(1), 206–220. <https://doi.org/10.1520/ACEM20170141>
- Qiao, C., Coyle, A., Isgor, O., & Weiss, W. (2018). Prediction of chloride ingress in saturated concrete using formation factor and chloride binding isotherm. *Advances in Civil Engineering Materials*, 7(1), 206–220. <https://doi.org/10.1520/ACEM20170141>
- Qiao, C., Moradillo, M. K., Hall, H., Ley, M. T., & Weiss, W. J. (2018). Electrical resistivity and formation factor of air-entrained concrete. *ACI Structural and Materials Journal*, 116(3). <https://doi.org/10.14359/51714506>
- Rajabipour, F., Weiss, J., Shane, J. D., Mason, T. O., & Shah, S. P. (2005, October 1). Procedure to interpret electrical conductivity measurements in cover concrete during rewetting. *Journal of Materials in Civil Engineering*, 17, 586–594. [https://doi.org/10.1061/\(ASCE\)0899-1561\(2005\)17:5\(586\)](https://doi.org/10.1061/(ASCE)0899-1561(2005)17:5(586))
- Sant, G., Rajabipour, F., & Weiss, W. J. (2008). The influence of temperature on electrical conductivity measurements and maturity predictions in cementitious materials during hydration. *Indian Concrete Journal*, 82(4), 7–16.
- Spragg, R. P. (2013). *The rapid assessment of transport properties of cementitious materials using electrical methods* [Master's thesis, Purdue University]. <https://docs.lib.purdue.edu/dissertations/AAI1549494/>
- Spragg, R. P., Castro, J., Nantung, T., Paredes, M., & Weiss, W. J. (2011). *Variability analysis of the bulk resistivity measured using concrete cylinders* (Joint Transportation Research Program Publication No. FHWA/IN/JTRP-2011/21). West Lafayette, IN: <https://doi.org/10.5703/1288284314646>
- Spragg, R., & Weiss, W. J. (2016). Chapter 11: Assessing a concrete's resistance to chloride ion ingress using the formation factor. In Amir Porsae (Ed.) *Corrosion of Steel in Concrete Structures* (1st ed., pp. 211–238). <https://doi.org/10.1016/C2014-0-01384-6>

- Spragg, R., Villani, C., & Weiss, W. J. (2016). Electrical properties of cementitious systems: Formation factor determination and the influence of conditioning procedures. *Advances in Civil Engineering Materials*, 5(1), 124–148. <https://doi.org/10.1520/ACEM20150035>
- Spragg, R., Villani, C., Snyder, K., Bentz, D., Bullard J. W., & Weiss, W. J. (2013). Factors that influence electrical resistivity measurements in cementitious systems. *Transportation Research Record: Journal of the Transportation Research Board*, 2342(1), 90–98. <https://doi.org/10.3141/2342-11>
- Weiss, W. J., Barrett, T. J., Qiao, C., & Todak, H. (2016). Toward a specification for transport properties of concrete based on the formation factor of a sealed specimen. *Advances in Civil Engineering Materials*, 5(1), 179–194. <https://doi.org/10.1520/ACEM20160004>
- Weiss, W. J., Barrett, T., Qiao, C., & Todak, H. (2016). Toward a specification for transport properties of concrete based on the formation factor of a sealed specimen. *Advances in Civil Engineering Materials*, 5(1), 179–194. <https://doi.org/10.1520/ACEM20160004>
- Weiss, W. J., Ley, T. M., Isgor, O. B., & Van Dam, T. (2017). Toward performance specifications for concrete durability: Using the formation factor for corrosion and critical saturation for freeze-thaw. In *TRB 96th Annual Meeting Compendium of Papers*. Transportation Research Board.

## About the Joint Transportation Research Program (JTRP)

On March 11, 1937, the Indiana Legislature passed an act which authorized the Indiana State Highway Commission to cooperate with and assist Purdue University in developing the best methods of improving and maintaining the highways of the state and the respective counties thereof. That collaborative effort was called the Joint Highway Research Project (JHRP). In 1997 the collaborative venture was renamed as the Joint Transportation Research Program (JTRP) to reflect the state and national efforts to integrate the management and operation of various transportation modes.

The first studies of JHRP were concerned with Test Road No. 1 — evaluation of the weathering characteristics of stabilized materials. After World War II, the JHRP program grew substantially and was regularly producing technical reports. Over 1,600 technical reports are now available, published as part of the JHRP and subsequently JTRP collaborative venture between Purdue University and what is now the Indiana Department of Transportation.

Free online access to all reports is provided through a unique collaboration between JTRP and Purdue Libraries. These are available at <http://docs.lib.purdue.edu/jtrp>.

Further information about JTRP and its current research program is available at <http://www.purdue.edu/jtrp>.

## About This Report

An open access version of this publication is available online. See the URL in the citation below.

Weiss, J. W., Qiao, C., Isgor, B., & Olek, J. (2020). *Implementing rapid durability measure for concrete using resistivity and formation factor* (Joint Transportation Research Program Publication No. FHWA/IN/JTRP-2020/08). West Lafayette, IN: Purdue University. <https://doi.org/10.5703/1288284317120>